Mequindox induces apoptosis, DNA damage, and carcinogenicity in Wistar rats

Qianying Liu[a,1], Zhixin Lei[b,1], Changqin Gu[c], Jingchao Guo[d], Huiru Yu[d], Zainab Fatima[d], Kaixiang Zhou[d], Muhammad A.B. Shabbir[d], Muhammad Kashif Maan[d], Qinghua Wu[e,f], Shuyu Xie[d,**], Xu Wang[d], Zonghui Yuan[a,d,*]

[a] National Reference Laboratory of Veterinary Drug Residues (HZAU), MAO Key Laboratory for Detection of Veterinary Drug Residues, China
[b] Department of Pharmaceutics, College of Pharmacy, University of Minnesota, Minneapolis, MN, USA
[c] A Department of Veterinary Medicine, Huazhong Agricultural University, Wuhan 430070, Hubei, China
[d] MOA Laboratory for Risk Assessment of Quality and Safety of Livestock and Poultry Products, Huazhong Agricultural University, Wuhan, Hubei, 430070, China
[e] College of Life Science, Yangtze University, Jingzhou, China
[f] Center for Basic and Applied Research, Faculty of Informatics and Management, University of Hradec Kralove, Hradec Kralove, Czech Republic

ARTICLE INFO

ABSTRACT

Mequindox (MEQ) is a synthetic antibacterial agent. Recent studies showed that MEQ and its primary metabolites exhibit strong genotoxicity to mammalian cells, and MEQ induced carcinogenicity in mice. These findings suggest that chronic exposure to MEQ could lead to an increased risk of cancer later in life. In the present study, four groups of Wistar rats (55 rats/sex/group) were fed with diets containing MEQ (0, 25, 55, and 110 mg/kg) for 2 years. The results showed that the hematological system, liver, kidneys, and adrenal glands, as well as the developmental and reproductive systems, were the main targets for MEQ. Liver toxicity mediated by MEQ was associated with apoptosis and the nuclear factor κB (NF-κB) signaling pathway. In addition, MEQ increased the incidence of tumors in rats. Phosphorylated histone H2AX (γ-H2AX) is identified as a biomarker of cellular response to DNA double-strand breaks (DSB). Our data demonstrated that γ-H2AX expression was significantly increased in tumors. Thus, high levels of DSB might be responsible for carcinogenesis in rats, and further investigation is absolutely required to clarify the exact molecular mechanisms for carcinogenicity caused by MEQ *in vivo*.

1. Introduction

Quinoxaline, a nitrogen heterocyclic compound, has been used in advanced drug discovery stages as an antitumor agent, HIV-1 reverse transcriptase inhibitor, plant growth regulator, fungicide, insecticide, herbicide, fluorescent probe, and dye intermediate (https://www.ncbi.nlm.nih.gov/pubmed/?term=Mfuh%20AM%5bAuthor%5d&cauthor=true&cauthor_uid=26087764.Mfuh and Larionov, 2015; Marzaro et al., 2007; He et al., 2012; Khier et al., 2010; Messenger and Rundegren, 2004). Quinoxaline-di-*N*-oxides (QdNOs), acting as inhibitors of DNA synthesis, have a wide range of biological properties (Carta et al., 2005; Cheng et al., 2015; Huang et al., 2015; Vicente et al., 2009; Liu et al., 2017a, 2018c). Owing to strong antimicrobial activity and ability to

ameliorate intestinal microflora and improve protein utilization *in vivo*, five QdNOs of carbadox (CBX), olaquindox (OLA), quinocetone (QCT), cyadox (CYA), and mequindox (MEQ) have been used as growth promoters in livestock and poultry farming (Liu et al., 2016; Liu et al., 2017a, b, c).

MEQ, a relatively new compound in QdNOs, was developed by the Lanzhou Institute of Animal Husbandry and Veterinary Drugs at the Chinese Academy of Agricultural Sciences (Ding et al., 2012; Ihsan et al., 2011; Ihsan et al., 2013a; Liu et al., 2017c, d). It was widely used in food-producing animals in China due to its strong inhibitory effect against *Treponeme, Pasteurella, Escherichia coli, Staphylococcus aureus*, and *Salmonella* sp. (Ding et al., 2012; Ihsan et al., 2011; Ihsan et al., 2013a; Liu et al., 2017c, d). However, the use of MEQ has raised serious

---

concerns about the health effects. Previous studies suggested that MEQ caused an adverse effect on pigs and chickens during clinical use (Chun, 2005; Hongxia et al., 2005; Ihsan et al., 2010). Chronic exposure to MEQ induced toxicity to the adrenal (Huang et al., 2009), endocrine, and reproductive systems in Wistar rats (Ihsan et al., 2011). In the chronic 180-day administration of MEQ (55, 110, and 275 mg/kg), MEQ invoked oxidative stress in the liver and kidney of rats (Huang et al., 2009, 2010b). After exposure to MEQ (275 mg/kg) for 90 days, a reduction in body weight, and obvious histological changes in liver and adrenal gland, were observed (Ihsan et al., 2010). Some recent studies also suggested that MEQ invoked genotoxicity and carcinogenicity (Liu et al., 2018a) and induced toxicity to liver, testis, and kidney in mice (Liu et al., 2017b, c, d; Liu et al., 2018b).

High prediction of genotoxicity for carcinogenicity has been well documented in extensive reviews (Brambilla and Martelli, 2007; Brambilla and Martelli, 2009; Brambilla et al., 2010; Liu et al., 2017e). The use of compounds with confirmed genotoxicity was banned in humans, except for some special drugs (ICH S2B. 2012; Liu et al., 2017e). Some studies suggested that QdNOs has numerous degrees of genetic toxicity. For example, CBX (WHO, 1991a) and OLA (WHO, 1991b) exhibited an obvious genotoxicity in bacterial and mammalian cells (Ihsan et al., 2013a, b; Chen et al., 2009; Hao et al., 2006). QCT increased micronuclei formation in human hepatocyte L02 and HepG2 cells (Dai et al., 2015; Jin et al., 2009) and invoked DNA fragmentation and reactive oxygen species (ROS) generation in human lymphocytes (Yang et al., 2013). Some studies reported that MEQ increased micronucleus formation in mice and caused chromosomal aberrations in V79 cells (Liu et al., 2016). *N*1-desoxymequindox (*N*1-MEQ) and bidesoxy-mequindox (B-MEQ) (Fig. 1), two primary metabolites of MEQ, exhibited genotoxicity in a set of genotoxicity tests (Liu et al., 2016). Compared with CBX, a higher mutagenicity of MEQ to mammalian cells was found *in vitro* and *in vivo* tests (Ihsan et al., 2013a). CBX and bidesoxy-carbadox (B-CBX) (Fig. 1) were proved to be carcinogens (Ihsan et al., 2013a, b; WHO, 1991a, b; Liu et al., 2016), and therefore, CBX was prohibited for use in food-producing animals by the Health Department of Canada and Commission of the European Community (Liu et al., 2017a; Wu et al., 2007). A recent study showed that MEQ induced genotoxicity and carcinogenicity in mice (Liu et al., 2018a).

Based on this information, the general and genetic toxicity studies indicated that people who have taken MEQ could be at increased risk of cancer later in life. It was recommended by regulatory agencies that genotoxicity testing be performed prior to commercialization (VICH, 2000; FDA, 2000a,b,c; ICH, 2012). A long-term carcinogenicity study is required for the pharmaceuticals that are in continuous clinical use for at least 6 months, or intermittent in a chronic recurrent condition (Snyder and Green, 2001). Considering that MEQ is intended for chronic use and its structural analogues like CBX and OLA are regarded as carcinogens, the carcinogenicity study of MEQ is immediately needed. Herein, a combined dietary chronic toxicity and carcinogenicity study in Wistar rats was performed. Formation of γ-H2AX in some tumors of rats treated with MEQ was also detected by immunohistochemistry to provide a complete toxicity spectrum of MEQ.

2. Materials and methods

2.1. Test material

MEQ ($C_{11}H_{10}N_2O_3$, CAS No: 60875-16-3, purity 99.5%) was supplied by the Institute of Veterinary Phamaceuticals, Huazhong Agricultural University (Wuhan, P.R. China). NF-κB p65 (D14E12) XP® Rabbit mAb, Cleaved-Caspase-3 (Asp175) antibody and Phospho-Histone H2A.X (Ser139) (20E3) Rabbit mAb were purchased from Cell Signaling Technology (U. S. A). All the other chemicals were of analytical grade.

2.2. Animals and diet preparation

Two hundred twenty female and 220 male specific pathogen-free Wistar rats (5–6 weeks old, weighing 140–180 g) were procured from the Center of Laboratory Animals of Hubei Province, Wuhan, P.R. China. Individual body weights of rats were within ± 20% of average. The study was approved by the Ethical Committee of the Faculty of Veterinary Medicine (Huazhong Agricultural University). Use of animals was in compliance with the National Institutes of Health (NIH) publication, "The Development of Science Based Guidelines for Laboratory Animal Care" (NRC, 2004).

2.3. Experimental design

According to the Organization for Economic Cooperation and Development (OECD) Guideline 453, US Food and Drug Administration (FDA) Redbook 2000 (FDA, 2000a, b, c) and Procedures for toxicological assessment of food in China, the high dose should cause a certain toxic effect but not produce death or severe suffering; the low dose was recommended to be 1 to 3 times the clinical dose with no toxic effect (GB15193.17, 2003; OECD, 2009). In a previous study, an increased level of potassium (K^+) in plasma without growth inhibition was observed when rats were fed MEQ at 110 mg/kg as part of their diet (Ihsan, 2011). A dose of 55 mg/kg as part of the diet was selected because it is the normal concentration of OLA permitted in food. The medium dosage of 55 mg/kg is within 2–4 times the minimal dose (25 mg/kg). Therefore, dose levels of 25, 55, and 110 mg/kg were selected in this study.

The design of this carcinogenicity study is presented in Table 1S. Rats were randomly assigned to four groups (55 rats/group/sex) based on their body weight, and each group of rat was fed a basal diet mixed with 0, 25, 55, or 110 mg/kg MEQ for a total period of 104 weeks. Forty rats (5 rats/group/sex) were euthanized at each time point of 26, 52, and 78 weeks. The remaining surviving rats were euthanized at 104 weeks.

2.4. Clinical pathology

Each rat was physically examined at least twice daily throughout the carcinogenicity study. Individual body weight data were obtained weekly, beginning from experimental diet administration through 13 weeks. Before necropsy at weeks 26, 52, 78, and 104, the fasted weights
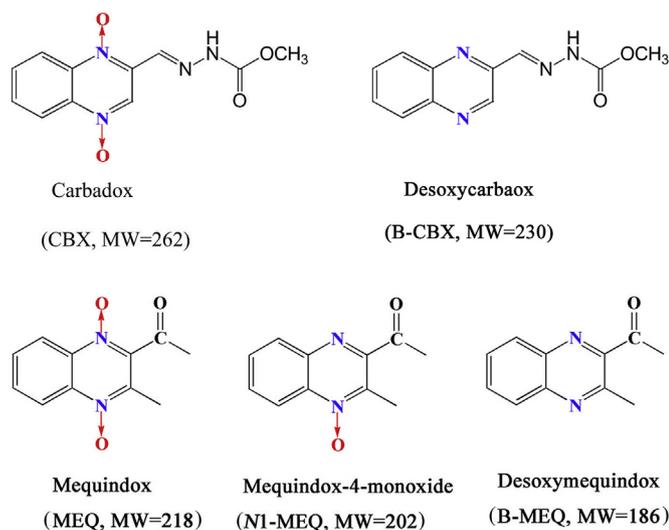

Fig. 1. The chemical structures of Carbadox (CBX), Desoxycarbadox (B-CBX), Mequindox (MEQ), Mequindox-4-monoxide (*N*1-MEQ) and Desoxymequindox (B-MEQ).

Carbadox
(CBX, MW=262)

Desoxycarbaox
(B-CBX, MW=230)

Mequindox
(MEQ, MW=218)

Mequindox-4-monoxide
(*N*1-MEQ, MW=202)

Desoxymequindox
(B-MEQ, MW=186)

were recorded. Individual body weight was calculated as described in the literature (Liu et al., 2017a).

Potassium ethylenediamine tetra-acetic acid (EDTA) was used as an anticoagulant in blood for hematology testing. Blood samples were placed in serum tubes at room temperature for approximately 30 min to obtain serum aliquots. After clotting, blood tubes were centrifuged at 3000 rpm for 10 min using the Himac CR 21 G centrifuge (Hitachi, Tokyo, Japan). The supernatants were decanted and stored at −20 °C for further serum biochemistry analysis.

2.5. Hematology and serum biochemistry

Hematological measurements and calculations were performed using the Coulter HmX *Hematology* Analyzer. The following 12 indicators were evaluated: red blood cell count (RBC), hemoglobin concentration (HGB), hematocrit (HCT), mean corpuscular volume (MCV), mean corpuscular hemoglobin (MCH), mean corpuscular hemoglobin concentration (MCHC), red cell volume distribution (RDW), plateletcrit (PCT), blood platelet count (PLT), mean platelet volume (MPV), platelet distribution width (PDW), and white blood cell count (WBC).

Serum biochemistry was assessed using the Synchron Clinical System *CX4*, and parameters included albumin (ALB), alkaline phosphatase (ALP), alanine aminotransferase (ALT), aspartate aminotransferase (AST), blood urea nitrogen (BUN), calcium ion (Ca^{++}), creatine kinase isoenzyme (CKM), chloride ion (CL$^-$), creatinine (CRE), glutamyl transpeptidase (GGT), glucose (GLU), globulin (GLB), high-density lipoprotein (HDL), lactate dehydrogenase (LDHD), low-density lipoprotein (LDL), phosphorus (PD), total bile acid (TBA), total bilirubin (TBIL), total cholesterol (TCHO), triglyceride (TG), total protein (TP), uric acid (UA), and urea (URE).

2.6. Necropsy and histopathological examinations

Complete necropsy and macroscopic examinations were conducted for each rat. Organs and tissues, including brain, heart, lungs, kidneys, liver, spleen, adrenal glands, testes (male), uterus (female), and ovary (female) were weighed separately to calculate organ weight per 100 g body weight (relative organ weight).

A microscopic examination was conducted on gross lesions and tissues from all rats. Histopathological examination was conducted using a routine paraffin embedding technique. Sections (5-μm thick) were stained with hematoxylin and eosin (H&E), and then morphological alterations were examined under light microscopy.

2.7. TUNEL assay

Rat livers were prepared on 4-μm paraffin sections using antigen retrieval for 10 min of boiling. The sections were permeabilized with 0.1% Triton X-100 after fixation. Samples were then stained with 1 μg/mL 4,6-diamino-2-phenylindole (DAPI) for 30 min after incubation with a terminal deoxynucleotide transferase-mediated dUTP nick end labeling (TUNEL) reagent containing terminal deoxynucleotidyl transferase and fluorescent isothiocyanate dUTP. Liver samples were analyzed in a drop of phosphate-buffered saline (PBS) under a fluorescence and ultraviolet light microscope.

2.8. Immunohistochemical assay

Liver samples and tumor tissues were dissected and fixed. Then, they were placed in a 58 °C environment for 10 min, followed by deparaffinization in xylol and rehydration in alcohol. The endogenous peroxidase was blocked with a 3% hydrogen peroxide solution for 30 min, and then washed. Slides were subjected to steam heat recovery (95 °C −100 °C for 30 min) washed with PBS, and incubated with 5% bovine serum albumin (BSA) at 37 °C for 1 h. After that, the glass slides of tumor samples were incubated with primary antibodies (γ-H2AX,

1:480), and the liver samples were incubated with primary antibodies (NF-κB, 1:800; cleaved Caspase-3, 1:300), according to the manufacturers' instructions overnight at 4 °C. Negative controls were processed without using the primary antibodies. The glass slides were then washed and incubated with the biotinylated secondary antibody for 1 h at 37 °C. After washing, they were incubated with 0.1% domain antibody (DAB) solution. Glass slides were washed in distilled water, dehydrated in alcohol, diaphanized in xylol, and mounted on Entelan® for optic microscopy examination.

2.9. Immunofluorescence assay

Liver samples were placed on 4-μm paraffin sections using antigen retrieval for 10 min in 10 mM citrate buffer and were then fixed in 4% paraformaldehyde at −20 °C for 3 min. After washing, sections were permeabilized with 0.1% Triton X-100, exposed to the blocking solution, and incubated with primary antibodies NF-κB and cleaved Caspase-3 at 4 °C overnight. After washing, sections were incubated with secondary fluorescently labeled Dylight 594 antibodies for 45 min. Nuclei were stained using DAPI. Fluorescent images were taken using an AX70 wide field microscope (Olympus).

2.10. Statistical analysis

Statistical analyses were performed by comparing treatment groups with the control group using SPSS 15.0 software. Group differences were assessed by one-way analysis of variance (ANOVA) followed by the Tukey test. The Levene test was performed to examine variance homogeneity. If variance was homogeneous, the data were subjected to one-way ANOVA; if not, they were analyzed by Kruskal–Wallis nonparametric ANOVA. The incidences of histopathological lesions and tumor were evaluated with the Fisher exact test (Doi et al., 2006; Liu et al., 2017a). A two-sided level of statistical significance was preset at $p < 0.05$ or 0.01.

3. Results

3.1. Mortality, survival observation, and body weights

The survival data in the carcinogenicity study and body weights over 13 weeks are presented in Fig. 2S. The body weights after 13 weeks are presented in Fig. 1S. No obvious clinical signs were found in any group before 18 weeks. The death of rats was observed from week 18, and detailed information of accidental deaths is presented in Table 2S. The numbers of accidental deaths during the study were 16, 10, 12, and 15 in control, M25, M55, and M110, respectively. The numbers of survived rats in the MEQ-treated groups were slightly higher than that in the control group (Fig. 2S). After pathological examination, the rats were found to have died due to hepatitis, pneumonia, uterus suppuration, or enteritis (Table 2S). Therefore, the cumulative mortality was 18.2% (20/110), 12.7% (14/110), 14.5% (16/110), and 17.3% (19/110) for control, and in the M25, M55, and M110 groups, respectively.

Forty rats (5 rats/group/sex) were euthanized at each of the time points of 26, 52, and 78 weeks. Thus, the number of deaths and euthanizations at weeks 26, 52, and 78 were 24 (9 + 15), 20 (5 + 15), 22 (7 + 15), and 24 (9 + 15) for the control group, M25, M55, and M110 female groups; and 26 (11 + 15), 24 (9 + 15), 24 (9 + 15), and 25 (10 + 15) for the control group, M25, M55, and M110 male groups, respectively. Excluding accidental deaths and scheduled necropsy (26, 52, and 78 wk), the percentage of survival at final scheduled necropsy (104 wk) was 56.4% (31/55), 63.6% (35/55), 60.0% (33/55), and 56.4% (31/55) for control, M25, M55, and M110 female groups, respectively. For males, the percentage of survival at final scheduled necropsy (104 wk) was 52.7% (29/55), 56.4% (31/55), 56.4% (31/55), and 54.5% (30/55) for control, and M25, M55, and M110 groups,

respectively.

Body weights in the MEQ female groups were lower than those in the control group, except in the M55 female group at the 3rd, 12th, and 13th weeks. Body weights in female rats at the 9th week were controls > M25 > M110 > M55. Excluding the aforementioned weeks, body weights in female rats were controls > M55 > M110 > M25. In male rats, body weights in the control group were higher than those in the MEQ-treated groups at the 2nd to 11th and 13th weeks. The trend of body weight was controls > M25 > M55 > M110 at 4th, 5th, 7th, and 10th weeks; controls > M55 > M25 > M110 at 2nd, 3rd, and 8th weeks; controls > M25 > M110 > M55 at 6th and 13th weeks. These results suggest that MEQ reduced the body weight of rats at tested concentrations.

3.2. Hematological examination

The hematological changes in the carcinogenicity study are presented in Fig. 3S. At the 26th week, a significant increase of RDW was found in the M55 mg/kg male group. In female rats at the 52 nd week, markedly changed levels of WBC and MCHC were noted in all MEQ-treated groups; a significant decrease in PLT was observed in M25 and M110 groups. In male rats at the 52 nd week, significant increases in RBC, MCHC, PLT, and PCT were noted in all MEQ-treated groups; significant increases in HCT and MPV were found in the M25 and M55 groups. At the 78th week, marked changes in WBC, RBC, and HGB were noted in all MEQ female groups; significant increases in WBC and HCT in the M25 and M55 groups, respectively, were found in both genders; significant decreases in MCH, MCHC, PLT, and PCT were found in M25 male rats. A significant increase in PLT and a significant decrease in MPV were observed in M25 and M110 female groups. A significant change in MCH and PLT was observed in the M25 group. At the 104th week, there was a significant decrease of MCHC in the M55 female group and the M25 male group, respectively. A significant decrease of MCV and significant increase of RDW were noted in the MEQ-treated groups at the 104th week. A significantly changed WBC was found in the M55 and M110 groups at the 104th week. A significantly decreased PCT was found in the M110 group at the 104th week.

3.3. Biochemical changes

The biochemical changes in our carcinogenicity study are presented in Fig. 4S. At the 26th week, significantly changed levels of GGT, GLU, ALB, ALP, ALT, AST, and CRE were noted in M110 female rats; a significant increase of TBA was observed in MEQ-treated male rats; significant increases in GGT, GLU, ALB, ALP, AST, and CL⁻ were noted in M55 male rats.

At the 52 nd week in female rats, significant increases in URE and GGT were found in the MEQ-treated groups; significant changes of UA, TP, ALP, ALT, TG, and CL⁻ were observed in the M110 group. At the 52 nd week in male rats, significant changes of UA, ALB, ALP, LDHD, and ALT were noted in the M110 group. In the M55 and M110 groups at the 52th week, there were significant changes of URE, GLU, and TP in the male rats, and a significant increase of URE in the female and male rats. At the 78th week, compared with the control group, there were significant increases in TCHO and ALB in the female groups, and significant changes of TCHO and TP in the MEQ-treated male groups. In the M55 and M110 groups at the 78th week, significant increases in ALP and TBIL were observed in female rats, and significant increases in TBIL and GLU in male rats, respectively. In M110 at the 78th week, there were significant changes of GLU and TP in female rats, and significant increases in ALP and CRE in male rats.

Compared with controls, a significant increase of AST was noted in both genders at the 104th week. In females, significant increases in ALB and TBA, and significant decreases in TG and Ca²⁺, were found in the M110 group at the 104th week; significant increases in GLU and a

significant decrease in TP were noted in the M55 group at the 104th week. In males, there was a significant decrease of TP, and significant increases in CRE, TBA, and GLU in the M110 group at the 104th week; a significant increase of LDHD was noted in the M55 group at the 104th week.
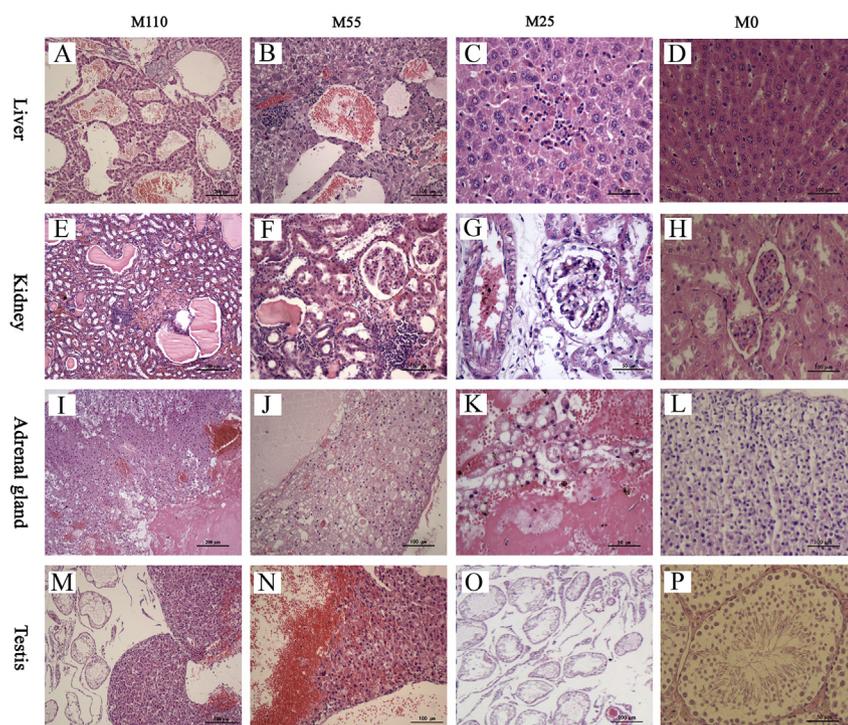
3.4. Organ weights and relative organ weights

In the females, there was a significant decrease in heart weight in the M110 group, and a significant decrease in liver and kidney weights in the MEQ-treated groups at the 26th week (Fig. 5S). A significant decrease in testis weight was noted in the M110 group at the 26th week. There was a significant increase in adrenal weight, and significant decreases in liver, lungs, and kidney weights in the M110 female group at the 52 nd week (Fig. 5S). At the 78th week, significant increases in heart and testis weight were observed in the M55 and M25 male groups, respectively; significant decreases in kidney and adrenal weights were found in the M55 female group; a significant decrease in brain weight was noted in the M110 female group (Fig. 5S). In females at the 104th week, significant decreases in spleen and brain weight, and significant decrease in kidney weight were observed in the MEQ-treated groups and the M110 group, respectively (Fig. 5S). In the males at the 104th week, there were significant increases in heart and liver weight in the M25 and M55 groups; significant increases in spleen and adrenal weights in the M55 group; and significant decreases in lung and kidney weights in the M25 group (Fig. 5S).

In females at the 26th week, we found a significant increase in the relative organ weight of the brain and a significant decrease in the relative organ weight of the liver in the M110 and M25 groups, respectively. A significant decrease in relative organ weights of the adrenal glands was found in M110 male rats at the 26th week (Fig. 6S). A significant decrease in the relative organ weight of lungs in the M55 and M110 groups, and significant decreases in relative organ weights of the liver and adrenal glands in the M110 group were observed in female rats at the 52 nd week (Fig. 6S). A significant increase of relative organ weight of the brain in the M25 group, and significant increases in relative organ weight of the adrenals and testis in the M110 group were noted in male rats at the 52 nd week (Fig. 6S). In the M55 group at the 78th week, a significant decrease in relative organ weight of adrenals was found in male rats, whereas significant decreases in relative organ weight of the kidneys and adrenals were noted in female rats (Fig. 6S). At the 104th week, a significant increase in relative organ weight of the lungs was observed in the M25 male group (Fig. 6S). In females, there were significant decreases in relative organ weights of the spleen and brain in all MEQ-treated groups at the 104th week, and a significant decrease of relative organ weight of the kidney was observed in the M55 and M110 groups at the 104th week (Fig. 6S).

3.5. MEQ induced toxicity to liver, kidney, adrenal gland, and testis in rats

At the 26th week, no obvious pathological findings were observed in the M25, M55, and control groups, whereas slight enlargement of liver cells occurred in some rats in the M110 group. At the 52nd, 78th, and 104th weeks, significant histopathological changes in liver, kidney, adrenal gland, and testis were observed in the MEQ-treated groups. At scheduled necropsy (104th week), dilatation and vacuolization of the central hepatic sinus with a large number of blood cells, proliferation of bile duct, neutrophilic infiltrate, and degeneration and necrosis of hepatic cells were observed in the liver of rats in the MEQ-treated groups (Fig. 2); aggregation of lymphocyte cells and infiltration of melanocytes in renal interstitial; degeneration and necrosis of renal tubular epithelial cells; formation of protein casts in tubular lumen; and expansion of glomerular capillaries were found in kidney in the MEQ-treated groups (Fig. 2). Vacuolization of cytoplasm in adrenocortical cells; formation of a large cystoid structure filled with a thin protein-like substance in deep cortex of adrenocortical and medulla; massive haemorrhage and

Fig. 2. Selected microphotographs of liver, kidney, adrenal gland and testis following dietary exposure to MEQ in the carcinogenicity tests (400 ×, 200 ×, 100 ×). (A) Liver from the M110 mg/kg group showing dilatation and vacuolization of the central hepatic sinus with a large number of blood cells and the proliferation of bile duct (100 ×); (B) Liver from the M55 mg/kg group showing aggregation of lymphocyte into a group and necrosis of hepatic cells (200 ×); (C) Liver from the M25 mg/kg group showing neutrophilic infiltrate, and swelling and degeneration of hepatic cells (400 ×); (D) Liver from the control group (200 ×); (E) Kidney from the M110 mg/kg group showing aggregation of lymphocyte cells and infiltration of melanocytes in renal interstitial (100 ×); (F) Kidney from the M55 showing degeneration and necrosis of renal tubular epithelial cells (200 ×); (G) Kidney from the M25 mg/kg group showing formation of the protein casts in the tubular lumen and expansion of the glomerular capillaries (400 ×); (H) Kidney from the control group (200 ×); (I) Adrenal gland from the M110 mg/kg group showing vacuolization of cytoplasm in adrenocortical cells, formation of a large cystoid structure filled with a thin protein like substance in the deep cortex of adrenocortical and medulla (100 ×); (J) Adrenal gland from the M55 showing massive haemorrhage and congestion of the medulla (200 ×); (K) Adrenal gland from the M25 mg/kg group showing melanocytic infiltration in medullary cells (400 ×); (L) Adrenal gland from the control group (200 ×); (M) Testis from the M110 mg/kg group showing a large expanse of the vascular cavity filled with red cells or edema fluid in the center of the testis, and residual the outline of convoluted tubules (100 ×); (N) Testis from the M55 mg/kg group showing cell proliferation around peripheral blood vessel (200 ×); (O) Testis from the M25 mg/kg group showing necrosis of spermatogonia and spermatocytes in the lumen (200 ×); (P) Testis from the control group (400 ×). (For interpretation of the references to color in this figure legend, the reader is referred to the Web version of this article.)

congestion of medulla and melanocytic infiltration in medullary cells in the adrenal gland were found in the MEQ-treated groups (Fig. 2). A large expanse of vascular cavity filled with red cells or edema fluid in the center of testis; residual outline of convoluted tubules; cell proliferation around peripheral blood vessel; vacuolization and decreased number of spermatogenic cells in the lumen; as well as necrosis of spermatogonia and spermatocytes were noted in the testis in the MEQ-treated groups (Fig. 2).

3.6. MEQ induced carcinogenicity in rats

The neoplastic findings and neoplasm incidence are presented in Table 1. In this carcinogenicity study, the total number of surviving rats was 371, including 181 males and 190 females. The number of surviving rats at final scheduled necropsy was 60, 66, 64, and 61 in control, M25, M55, and M110 groups, respectively. The rat tumors were mainly of eight types, including hepatocarcinoma (Fig. 3A), breast cancer (Fig. 3B), corticosuprarenaloma (Fig. 3C), hemangioma (Fig. 3D), brain cancer (Fig. 3E), pulmonary mesothelioma (Fig. 3F), mesonephroid carcinoma of the ovary (Fig. 3G), and melanoma (Fig. 3H).

3.7. MEQ induced apoptosis, γ-H2AX formation, and activation of the NF-κB pathway

TUNEL staining was conducted to investigate apoptosis of the liver induced by MEQ, which showed that obvious apoptosis was found in the MEQ-treated groups (Fig. 4). Cleaved caspase-3 is a well-characterized cell apoptotic marker; the protein level of cleaved Caspase-3 was detected by immunofluorescence assay (Fig. 5), indicating that compared with the control group, treating with MEQ caused increased cleaved Caspase-3 expression. In addition, immunofluorescence assay suggested that the protein level of NF-κB was increased in the MEQ-treated groups (Fig. 5). Taken together, these results suggested that

apoptosis and NF-κB pathway are associated with liver toxicity induced by MEQ.

γ-H2AX formation in hepatocarcinoma, hemangioma, pulmonary mesothelioma, and corticosuprarenaloma of rats was investigated by immunohistochemistry (Fig. 6). γ-H2AX-positive cells with characteristic intranuclear dot-like foci were distributed in tumor tissues, whereas γ-H2AX formation was rarely observed in the control groups. Through quantitative analysis (Fig. 6), we found that MEQ induced significant increases in the expression of γ-H2AX in hepatocarcinoma, hemangioma, pulmonary mesothelioma, and corticosuprarenaloma compared with controls. This finding demonstrated that DNA damage was involved in carcinogenicity induced by MEQ.

4. Discussion

MEQ is a synthetic antibacterial agent widely used in livestock because of strong inhibitory activity against both gram-positive and gram-negative bacteria (Li et al., 2014; Liu et al., 2016; Wu et al., 2012). General toxicity studies demonstrated that MEQ induced toxicity to adrenal (Huang et al., 2009), testis (Ihsan et al., 2011; Liu et al., 2017c, d), kidney, and liver (Huang et al., 2010a; Liu et al., 2017b). The mutagenic and carcinogenic potential restricts the wide use of QdNOs as a pharmaceutical building block. For example, CBX (WHO, 1991a) and OLA (WHO, 1991b) had been prohibited in food-producing animals due to mutagenic and carcinogenic effects (Liu et al., 2016; Wu et al., 2007). A recent study showed that MEQ induced genotoxicity and carcinogenicity in mice (Liu et al., 2018a). These findings suggest that chronic exposure to MEQ could place people at increased risk of cancer later in life. In the present study, MEQ induced an adverse effect on hematology, liver, kidneys, and adrenal glands as well as the developmental and reproductive system. MEQ increased tumor incidence and γ-H2AX formation in rats. In addition, apoptosis and the NF-κB pathway were associated with liver toxicity mediated by MEQ. Our study found that MEQ was a genotoxic carcinogen to rats.

Table 1
Neoplastic findings and neoplasm incidence in carcinogenicity study of mequindox in rats.

Females	Control (n = 46)	M25 (n = 50)	M55 (n = 48)	M110 (n = 46)
Brain				
Ependymal tumor	0 (0.0%)	0 (0.0%)	1 (2.1%)*	0 (0%)
Liver				
Hepatocarcinoma	2 (4.3%)	8 (16.0%)*	9 (18.8%)*	8 (17.4%)*
Spleen				
Splenic hemangioma	1 (2.2%)	5 (10.0%)*	6 (12.5%)*	8 (17.4%)*
Lung				
Pulmonary mesothelioma	0 (0.0%)	6 (12.0%)*	6 (12.5%)*	5 (10.9%)*
Adenocarcinoma	2 (4.3%)	5 (10.0%)*	7 (14.6%)*	4 (8.7%)*
Uterus				
Uterine leiomyoma	1 (2.2%)	4 (8.0%)*	6 (12.5%)*	4 (8.7%)*
Ovary				
Mesonephroid carcinoma	0 (0.0%)	7 (14.0%)*	8 (16.7%)*	7 (15.2%)*
Subcutaneous				
Melanoma	0 (0.0%)	5 (10.0%)*	4 (8.3%)*	6 (13.0%)*
Breast fibroadenoma,	6 (13.0%)	10 (20.0%)*	9 (18.0%)*	8 (17.4%)*
Breast Tumor	1 (2.1%)	5 (10.0%)*	7 (14.6%)*	14 (29.2%)*
Adrenal gland				
Corticosuprarenaloma	0 (0%)	9 (18.0%)*	6 (12.5%)*	8 (17.4%)*
Males	**Control (n = 44)**	**M25 (n = 46)**	**M55 (n = 46)**	**M110 (n = 45)**
Liver				
Hepatocarcinoma	3 (6.8%)	11 (23.9%)*	9 (19.6%)*	8 (17.8%)*
Spleen				
Splenic hemangioma	2 (4.5%)	6 (13.0%)*	7 (15.2%)*	7 (15.6%)*
Testis				
Melanoma	4 (9.1%)	8 (17.4%)*	10 (21.7%)*	14 (31.1%)*
Lung				
Pulmonary mesothelioma	1 (2.3%)	6 (13.0%)*	8 (17.4%)*	9 (20.0%)*
Adenocarcinoma	2 (4.5%)	10 (21.7%)*	9 (19.6%)*	11 (24.4%)*
Subcutaneous				
Melanoma	2 (4.5%)	8 (17.4%)*	7 (15.2%)*	9 (20.0%)*
Intestinal				
Colon cancer	1 (2.3%)	1 (2.2%)	2 (4.3%)	0 (0%)
Adrenal gland				
Corticosuprarenaloma	0 (0.0%)	9 (19.6%)*	13 (28.3%)*	10 (22.2%)*

Note: *Significantly different from control group at $p < 0.05$ by Fisher exact test.
M, mequindox; M25, 25 mg/kg diet; M55, 55 mg/kg diet; M110, 110 mg/kg diet.

In the hematopoietic system, significant changes in hematological parameters of WBC, MCV, MCHC, RDW, and PCT were noted in the MEQ-treated groups at the 104th week, indicating that MEQ caused an adverse effect on the hematopoietic system in rats. However, hematological toxicity was not observed in rats after exposure to MEQ for 90 days (Ihsan et al., 2010). In the present study, there was only one parameter of RDW that significantly increased in the M55 male group at the 26th week, indicating that hematological toxicity increased with prolongation of MEQ administration. The current study suggests that the hematological system might be the target of MEQ after chronic exposure in rats. It was found that liver is one of the main target organs for toxicity mediated by CYA (Liu et al., 2018c), QCT (Liu et al., 2017c), and MEQ (Ihsan et al., 2010). The centrilobular liver cell necrosis, disorganized hepatic cord pattern, and cellular swelling were caused by MEQ in rats (Ihsan et al., 2010) and mice (Liu et al., 2017b). In the present study, significantly changed levels of ALB, AST, and CRE, as well as liver weights, were observed in week 104 in the MEQ-treated groups. These observations demonstrated that MEQ might be harmful to the liver. Histopathological examination indicated dilatation and vacuolization of the central hepatic sinus, proliferation of the bile duct,
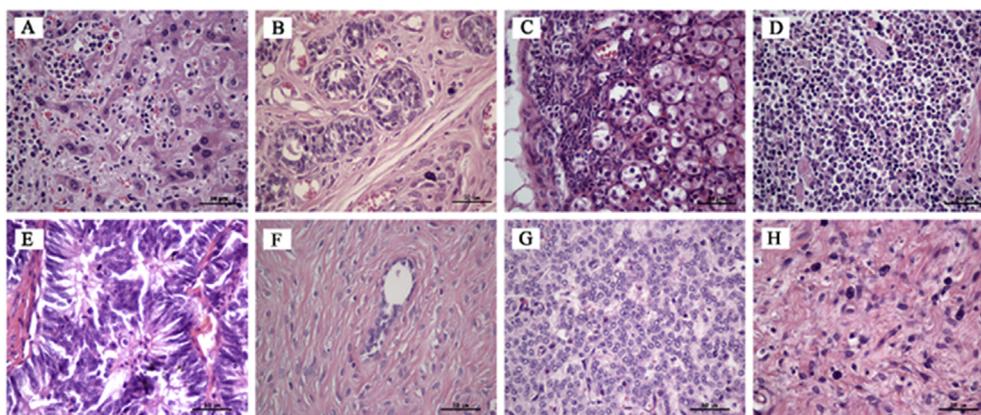

Fig. 3. Selected microphotographs of the identified neoplasm in the MEQ treated groups in the carcinogenicity study (400 ×). (A) Hepatocarcinoma; (B) Breast cancer; (C) Corticosuprarenaloma; (D) Haemangiomas; (E) Brain cancer; (F) Pulmonary mesothelioma; (G) Mesonephroid carcinoma of ovary; (H) Melanoma.
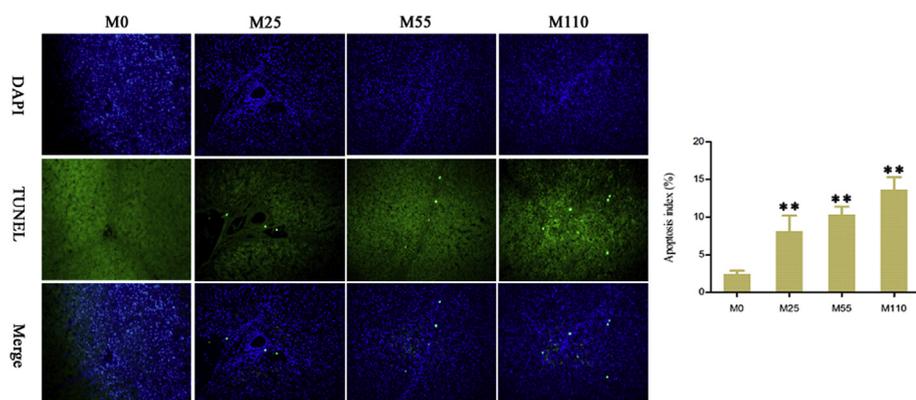
Fig. 4. TUNEL staining of liver tissue. Cell nuclei (Blue), TUNEL-positive cells (Green). (Scale bar = 50 μm). The green spots represent TUNEL-positive cells. (A) The liver from control group showing normal cells; (B, C and D) the livers from MEQ treated groups showing tissue lesion and apoptosis. (For interpretation of the references to color in this figure legend, the reader is referred to the Web version of this article.)

neutrophilic infiltrate and degeneration and necrosis of hepatic cells in the liver of rats in the MEQ-treated groups at the 104th week. In TUNEL staining analysis, obvious apoptosis was noted in the livers treated with MEQ. Cleaved Caspase-3 is a well-characterized cell apoptotic marker. NF-κB is reported to be involved in immunological and cellular detoxifying defense systems (Prasad et al., 2010; Yu et al., 2014; Ze et al., 2013). Our data indicated that MEQ invoked the expression of cleaved Caspase-3 and NF-κB in liver. Thus, our results not only confirmed the earlier finding that liver was a toxic target of MEQ, but also showed that apoptosis and the NF-κB pathway were involved in liver toxicity mediated by MEQ (Liu et al., 2017b; Ihsan et al., 2010).

The changed concentration of BUN is associated with the function of the kidneys and adrenal glands (Huang et al., 2010a, b). MEQ damaged the adrenal glands with decreased aldosterone concentration in plasma (Huang et al., 2010a) and reduced the output of adrenal aldosterone (Huang et al., 2010b). Previous studies reported adrenal toxicity in rats after administration of MEQ (Huang et al., 2009, 2010a; Ihsan et al., 2010). In the present study, a significant change in BUN in the 104th week was noted in the MEQ-treated groups, indicating that chronic injury in the kidneys and adrenal glands occurred. Histopathological changes in the kidneys and adrenal glands were also found in the MEQ-treated groups. Earlier studies found that MEQ led to obvious histological changes in the liver (Liu et al., 2017a), kidney (Liu et al., 2018b), and adrenal gland (Huang et al., 2009). Recently, we found that MEQ and its primary metabolites, N1-MEQ and B-MEQ, exhibited adrenal toxicity in H295R cells (Wang et al., 2016). Taken together, our data indicated that the liver, kidneys, and adrenal glands were the main target organs for MEQ in vivo.

In recent studies, a few toxicity-linked parameters, such as serum urea, Caspase-8, and GSH, were changed by MEQ in a non-dose-dependent manner (Liu et al., 2018b). The toxicity of MEQ to Na

concentration and relative brain weight in F1 rats were not dose-dependent (Liu et al., 2018a). These findings suggested hormesis in the toxicity induced by MEQ. In the present study, most of the indicators had no dose- and time-dependent changes in the hematological examination, biochemical changes, or organ weights, and the hormesis was suspected to account for these results.

Much evidence suggested that CBX and OLA had developmental and reproductive toxicities (Ihsan et al., 2013a; Liu et al., 2017c; WHO, 1991a, b). After exposure to CBX at 25 mg/kg/day, a teratogenic effect and significant decrease in fetal and maternal body weights were observed in rats (Yoshimura, 2002). OLA (5 mg/kg b.w./day) caused toxic effects in the testes of rats (WHO, 1991b). In addition, MEQ was found to damage the integrity of the blood-testis barrier (BTB) and inhibit spermatogenesis in mice (Liu et al., 2017c, d). In this study, significant histopathological alterations of testis, uterus, and ovary were observed in the MEQ-treated groups, indicating that MEQ had an adverse effect on the developmental and reproductive system. The present study is the first to report uterus and ovary toxicity induced by MEQ, and the exact molecular mechanism should be investigated. Histopathological examination showed serious lesions in the testis of rats, including vacuolization and decreased number of spermatogenic cells in the lumen, cell proliferation around peripheral blood vessels mixed with a large number of blood cells, and necrosis of spermatogonia and spermatocytes in the lumen. Regarding the mechanisms of testis toxicity, it was illustrated that oxidative stress, mitochondrion dysfunction, and demolished integrity of BTB were all involved in the reproductive toxicity mediated by MEQ in vivo (Liu et al., 2017c, d). Due to serious testis damage in rats, further study is undeniably required to clarify the adverse effect of MEQ on the fertility of animals.

As reported, CBX and B-CBX had genotoxic and carcinogenic effects (Ihsan et al., 2013b, c; Zhao et al., 2014). A treatment-related increase
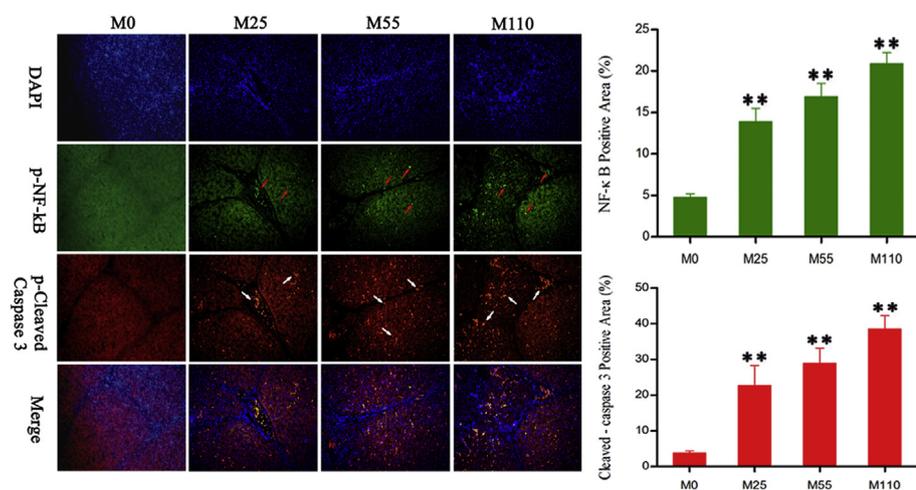

Fig. 5. Immunofluorescence for NF-κB and cleaved - caspase 3 (Scale bar = 50 μm). Blue spots represent cell nuclei, green spots represent NF-κB staining and red spots represent cleaved - caspase 3 staining. The integrated option density (IOD) of DAPI was used as an internal control. A indicates the liver from the control group, and the B, C and D indicate the livers from M25, M55 and M110 groups, respectively. (For interpretation of the references to color in this figure legend, the reader is referred to the Web version of this article.)
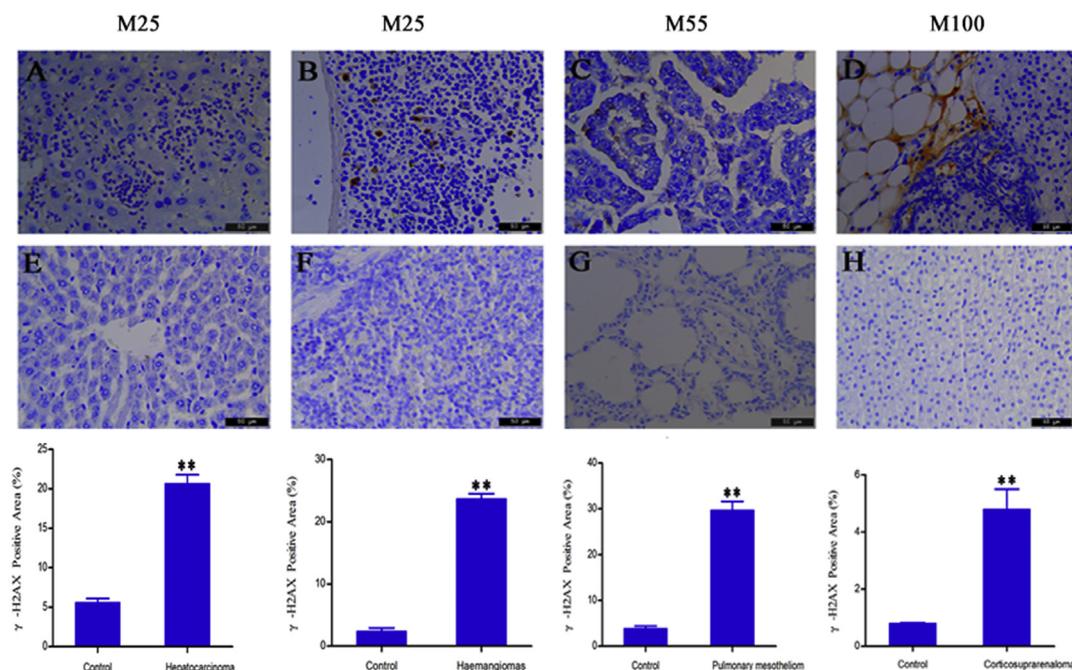
Fig. 6. The protein expression of γ-H2AX was detected by immunohistochemical assays (Scale bar = 50 μm). The positive reaction of anti-γ-H2AX antibody was brown. (A–D) Areas of hepatocarcinoma, haemangiomas, pulmonary mesothelioma and corticosuprarenaloma in the MEQ treated groups showing several brown-colored γ-H2AX-positive nuclei. (E–H) Areas of liver, spleen, lung and adrenal gland showing only blue-stained γ-H2AX-negative nuclei. (For interpretation of the references to color in this figure legend, the reader is referred to the Web version of this article.)

in total tumors was found in rats and, interestingly, the lower tumor incidence was noted in the high-dose group of CBX (Stebbins and Coleman, 1967). It was suggested that hepatic injury was involved in observed nodular hyperplasia after treatment with CBX. In another study, CBX caused a large number of tumors (Sykora and Vortel, 1986). B-CBX was a potent hepatocarcinogen in rats and induced a dose-related increase in tumors, including hepatic tumors, subcutaneous fibromas, hemanigiomas, and mammary tumors (Reinert, 1976). B-CBX yielded positive responses in a cell transformation test on BALB/C Swiss 3T3 and caused chromosomal damage in rat bone marrow (Pfizer, 1975). Both CBX and B-CBX were confirmed as carcinogens that act by a genotoxic mechanism (JECFA, 2003). In the present study, increased tumor incidence was noted in the MEQ-treated groups when compared with the control group. The tumors were mainly of eight types, including hepatocarcinoma, breast cancer, corticosuprarenaloma, hemangioma, brain cancer, pulmonary mesothelioma, mesonephroid carcinoma of the ovary, and pigmented tumor. These results confirmed MEQ as a carcinogen in rats.

Phosphorylation of histone H2AX at serine 139 (producing γ-H2AX) is a well-established biomarker of DNA double-strand breaks (DSB) (https://www.ncbi.nlm.nih.gov/pubmed/?term=Azzar%C3%A0%20A%5bAuthor%5d&cauthor=true&cauthor_uid=28714549.Azzarà et al., 2017; Scarpato et al., 2011; https://www.ncbi.nlm.nih.gov/pubmed/?term=Toyoda%20T%5bAuthor%5d&cauthor=true&cauthor_uid=29143974.Toyoda et al., 2018; Redon et al., 2011). The number of γ-H2AX foci reflects approximately the number of nuclear DSB formed, and thus, γ-H2AX has been used in genotoxicity screening for chemical materials (Khoury et al., 2016; Nikolova et al., 2014). γ-H2AX surrounds the site of DSB (γ-H2AX foci), leading to aggregation of repair proteins, and this process can be microscopically detected by immunohistochemistry (Redon et al., 2012; https://www.ncbi.nlm.nih.gov/pubmed/?term=Toyoda%20T%5bAuthor%5d&cauthor=true&cauthor_uid=29143974.Toyoda et al., 2018). Therefore, immunostaining of γ-H2AX is a useful tool to predict genotoxicity of chemicals (Nagelkerke and Span, 2016; Thompson et al., 2015; Toyoda et al., 2015). In the present study, γ-H2AX-positive cells were detected

in the hepatocarcinomas, corticosuprarenalomas, hemangiomas, and pulmonary mesotheliomas, indicating that MEQ exhibited genotoxicity in rats. Previous studies suggested that MEQ and its metabolites induced DNA strand breaks in HepG2 cells (Wang et al., 2015). MEQ increased micronucleus formation and caused chromosomal aberrations in V79 cells (Liu et al., 2016). Thus, our data illustrated that γ-H2AX formation might be responsible for carcinogenesis in rats, and further investigation is absolutely required to clarify the exact molecular mechanisms for carcinogenicity of MEQ *in vivo*.

A recent study found that B-MEQ and *N*1-MEQ were genotoxic in a set of four different short-term tests (Liu et al., 2016). Hydrazine was a possible metabolite derived from cleavage of the CBX side chain. Oral administration of hydrazine produced a 100% incidence of lung tumors in Balb/c female mice at 1.13 mg/day for 46 weeks (Biancifiori and Ribacchi, 1962). In another study on Swiss mice, hydrazine induced 46% incidence of lung tumors versus 10% in controls (Roe et al., 1967). Quinoxaline-2-carboxylic acid (QCA) and methyl carbazate, another two primary metabolites of CBX, were reported to be non-carcinogens (JECFA, 2003; WHO, 1991a,b). No treatment-related genotoxicity or carcinogenicity was observed on QCA (Pfizer, 1975) and methyl carbazate (JECFA, 2003). OLA resulted in pulmonary adenoma and adrenal cortical adenoma in males, and pulmonary adenoma and ovarian granulosa cell tumors in females at 360 mg/kg in the diet (Steinhoff and Gunselmann, 1982). Benign fibromas of the skin were observed in Wistar rats after administration of OLA (400 mg/kg diet) for 78 weeks (Wang et al., 2011). CYA was not found to be genotoxic in mammalian cells (Liu et al., 2016), and also non-carcinogenic in Sprague-Dawley rats (Liu et al., 2017a). Considering the same quinoxaline ring presented in QdNOs, it was suspected that the side chains might play a critical role in genotoxicity and carcinogenicity of QdNOs. Further study should be conducted to find the origin of structure-genotoxicity and structure-carcinogenicity relationships of QdNOs, which would enable us to find ways to hinder a particular chemical event that leads to a formation of genotoxic and carcinogenic products.

Conflict of interest statement

The authors declare that there are no conflicts of interest.

Acknowledgements

Appendix A. Supplementary data

Supplementary data to this article can be found online at https://doi.org/10.1016/j.fct.2019.03.025.

Transparency document

Transparency document related to this article can be found online at https://doi.org/10.1016/j.fct.2019.03.025.

References

Azzarà, A., Chiaramonte, A., Filomeni, E., Pinto, B., Mazzoni, S., Piaggi, S., Angela Guzzardi, M., Bruschi, F., Iozzo, P., Scarpato, R., 2017. Increased level of DNA damage in some organs of obese Zucker rats by γ-H2AX analysis. Environ. Mol. Mutagen. 58 (7), 477–484.

Biancifiori, C., Ribacchi, R., 1962. Pulmonary tumour in mice induced by oral isoniazid and its metabolites. Nature 194, 488–489.

Brambilla, G., Martelli, A., 2007. Genotoxic and carcinogenic risk to humans of drug-nitrite interaction products. Mutat. Res. 635, 17–52.

Brambilla, G., Martelli, A., 2009. Update on genotoxicity and carcinogenicity testing of 472 marketed pharmaceuticals. Mutat. Res. 681, 209–229.

Brambilla, G., Mattioli, F., Robbiano, L., Martelli, A., 2010. Genotoxicity and carcinogenicity testing of pharmaceuticals: correlations between induction of DNA lesions and carcinogenic activity. Mutat. Res. 705, 20–39.

Carta, A., Corona, P., Loriga, M., 2005. Quinoxaline 1,4-dioxide: a versatile scaffold endowed with manifold activities. Curr. Med. Chem. 12, 2259–2272.

Chen, Q., Tang, S., Jin, X., Zou, J., Chen, K., Zhang, T., Xiao, X., 2009. Investigation of the genotoxicity of quinocetone, carbadox and olaquindox in vitro using Vero cells. Food Chem. Toxicol. 47, 328–334.

Cheng, G., Li, B., Wang, C., Zhang, H., Liang, G., Weng, Z., et al., 2015. Systematic and molecular basis of the antibacterial action of quinoxaline 1,4-di-N-oxides against Escherichia coli. PLoS One 10, e0136450.

Chun, C., 2005. Careful Use of Mequindox in Chicken. China Poultry 04. (Chinese article).

Dai, C., Tang, S., Li, D., Zhao, K., Xiao, X., 2015. Curcumin attenuates quinocetone-induced oxidative stress and genotoxicity in human hepatocyte L02 cells. Toxicol. Mech. Methods 25, 340–346.

Ding, H., Liu, Y., Zeng, Z., et al., 2012. Pharmacokinetics of mequindox and one of its major metabolites in chickens after intravenous, intramuscular and oral administration. Res. Vet. Sci. 93 (1), 374–377.

Doi, Y., Ichihara, T., Hagiwara, A., Imai, N., Tamano, S., Orikoshi, H., Ogasawara, K., Sasaki, Y., Nakamura, M., Shirai, T., 2006. A ninety-day oral toxicity study of a new type of processed gum Arabic, from Acacia tree (Acacia Senegal) exudates, in F344 rats. Food Chem. Toxicol. 44, 560–566.

FDA, 2000a. IV.C.5a. Chronic Toxicity Studies with Rodents, Redbook 2000: Toxicological Principles for the Safety Assessment of Food Ingredients. US Food and Drug Administration, Washington, D.C.

FDA, 2000b. IV.C.6. Carcinogenicity Studies with Rodents, Redbook 2000: Toxicological Principles for the Safety Assessment of Food Ingredients. US Food and Drug Administration, Washington, D.C.

FDA, 2000c. IV.C.7. Combined Chronic Toxicity/Carcinogenicity Studies with Rodents, Redbook 2000: Toxicological Principles for the Safety Assessment of Food Ingredients. US Food and Drug Administration, Washington, D.C.

GB15193.17, 2003. Chronic Toxicity and Carcinogencity Study. pp. 109–113.

Hao, L., Chen, Q., Xiao, X., 2006. Molecular mechanism of mutagenesis induced by olaquindox using a shuttle vector pSP189/mammalian cell system. Mutat. Res. 599, 21–25.

He, J., Feng, L., Li, J., Tao, R., Wang, F., Liao, X., Sun, Q., Long, Q., Ren, Y., Wan, J., He, H., 2012. Design, synthesis and biological evaluation of novel 2-methylpyrimidine-4-ylamine derivatives as inhibitors of Escherichia coli pyruvate dehydrogenase complex E1. Bioorg. Med. Chem. 20 (5), 1665–1670.

Hongxia, L., Wei, J., Guilan, Z., 2005. Mequindox poisioning; diagnosis and treatment. Livestock and Poultry. Industry 4, 54–55 (Chinese article).

Huang, X.J., Ihsan, A., Wang, X., et al., 2009. Long-term dose-dependent response of Mequindox on aldosterone, corticosterone and five steroidogenic enzyme mRNAs in the adrenal of male rats. Toxicol. Lett. 191 (2–3), 167–173.

Huang, X.J., Wang, X., Ihsan, A., Liu, Q., Xue, X.J., Su, S.J., Yang, C.H., Zhou, W., Yuan, Z.H., 2010a. Interactions of NADPH oxidase, renin-angiotensin-aldosterone system and reactive oxygen species in mequindox-mediated aldosterone secretion in Wistar rats. Toxicol. Lett. 198, 112–118.

Huang, X.J., Zhang, H.H., Wang, X., Huang, L.L., Zhang, L.Y., Yan, C.X., Liu, Y., Yuan, Z.H., 2010b. ROS mediated cytotoxicity of porcine adrenocortical cells induced by QdNOs derivatives in vitro. Chem. Biol. Interact. 185, 227–234.

Huang, Q., Ihsan, A., Guo, P., Luo, X., Cheng, G., Hao, H., Chen, D., Jamil, F., Tao, Y., Wang, X., Yuan, Z., 2015. Evaluation of the safety of primary metabolites of cyadox: acute and sub-chronic toxicology studies and genotoxicity assessment. Regul. Toxicol. Pharmacol. 74, 123–136.

ICH, 2012. Guidance for Industry Genotoxicity Testing and Data Interpretation for Pharmaceuticals Intended for Human Use.

Ihsan, A., 2011. Preclinical Toxicology of Mequindox. Ph.D. thesis. Huazhong Agricultural university, Wuhan.

Ihsan, A., Wang, X., Huang, X.J., Liu, Y., Liu, Q., Zhou, W., Yuan, Z.H., 2010. Acute and subchronic toxicological evaluation of Mequindox in Wistar rats. Regul. Toxicol. Pharmacol. 57, 307–314.

Ihsan, A., Wang, X., Liu, Z., Wang, Y., Huang, X., Liu, Y., Yu, H., Zhang, H., Li, T., Yang, C., Yuan, Z., 2011. Long-term mequindox treatment induced endocrine and reproductive toxicity via oxidative stress in male Wistar rats. Toxicol. Appl. Pharmacol. 252, 281–288.

Ihsan, A., Wang, X., Tu, H.G., et al., 2013a. Genotoxicity evaluation of Mequindox in different short-term tests. Food Chem. Toxicol. 51, 330–336.

Ihsan, A., Wang, X., Zhang, W., et al., 2013b. Genotoxicity of quinocetone, cyadox and olaquindox in vitro and in vivo. Food Chem. Toxicol. 59, 207–214.

JECFA, 2003. WHO FOOD ADDITIVES SERIES: 51. CARBADOX (Addendum). http://www.inchem.org/documents/jecfa/jecmono/v51je05.htm#2.2.

Jin, X., Chen, Q., Tang, S.S., Zou, J.J., Chen, K.P., Zhang, T., Xiao, X.L., 2009. Investigation of quinocetone-induced genotoxicity in HepG2 cells using the comet assay, cytokinesis-block micronucleus test and RAPD analysis. Toxicol. Vitro 23, 1209–1214.

Khier, S., Deleuze-Masquéfa, C., Moarbess, G., Gattacceca, F., Margout, D., Solassol, I., Cooper, J.F., Pinguet, F., Bonnet, P.A., Bressolle, F.M., 2010. Pharmacology of EAPB0203, a novel imidazo[1,2-a]quinoxaline derivative with anti-tumoral activity on melanoma. Eur. J. Pharm. Sci. 39 (1–3), 23–29.

Khoury, L., Zalko, D., Audebert, M., 2016. Complementarity of phosphorylated histones H2AX and H3 quantification in different cell lines for genotoxicity screening. Arch. Toxicol. 90, 1983–1995.

Li, J., Huang, L.L., Wang, X., et al., 2014. Metabolic disposition and excretion of quinocetone in rats, pigs, broilers, and carp. Food Chem. Toxicol. 69, 109–119.

Liu, Q., Zhang, J., Luo, X., Ihsan, A., Liu, X., Dai, M., Cheng, G., Hao, H., Wang, X., Yuan, Z., 2016. Further investigations into the genotoxicity of quinoxaline-di-N-oxides and their primary metabolites. Food Chem. Toxicol. 93, 145–157.

Liu, Q., Lei, Z., Cui, L., Zhang, J., Awais, I., Dai, M., Wang, X., Yuan, Z., 2017a. A two-year dietary carcinogenicity study of cyadox in Sprague-Dawley rats. Regul. Toxicol. Pharmacol. 87, 9–22.

Liu, Q., Lei, Z., Huang, A., Wu, Q., Xie, S., Awais, I., Dai, M., Wang, X., Yuan, Z., 2017b. Toxic metabolites, MAPK and Nrf2/Keap1 signaling pathways involved in oxidative toxicity in mice liver after chronic exposure to Mequindox. Sci. Rep. 7, 41854.

Liu, Q., Lei, Z., Dai, M., Wang, X., Yuan, Z., 2017c. Toxic metabolites, Sertoli cells and Y chromosome related genes are potentially linked to the reproductive toxicity induced by mequindox. Oncotarget 8, 87512–87528.

Liu, Q., Lei, Z., Huang, A., Lu, Q., Wang, X., Ahmed, S., Awais, I., Yuan, Z., 2017d. Mechanisms of the testis toxicity induced by chronic exposure to mequindox. Front. Pharmacol. 8, 679.

Liu, Q., Lei, Z., Zhu, F., Awais, I., Wang, X., Yuan, Z., 2017e. A novel strategy to predict carcinogenicity of antiparasitics based on a combination of DNA lesions and bacterial mutagenicity tests. Frontiers in public health 5, 288.

Liu, Q., Lei, Z., Wu, Q., Huang, D., Xie, S., Wang, X., Pan, Y., Yuan, Z., 2018a. Mequindox induced genotoxicity and carcinogenicity in mice. Front. Pharmacol. 9, 361.

Liu, Q., Lei, Z., Guo, J., Liu, A., Lu, Q., Fatima, Z., Khaliq, H., Shabbir, M.A.B., Maan, M.K., Wu, Q., Dai, M., Wang, X., Pan, Y., Yuan, Z., 2018b. Mequindox-induced kidney toxicity is associated with oxidative stress and apoptosis in the mouse. Front. Pharmacol. 9, 436.

Liu, Q., Lei, Z., Zhou, K., Yu, H., Liu, S., Sun, Q., Wang, X., Dai, M., Yuan, Z., 2018c. N-O reduction and ROS-mediated AKT/FOXO1 and AKT/P53 pathways are involved in growth promotion and cytotoxicity of cyadox. Chem. Res. Toxicol. 31 (11), 1219–1229.

Marzaro, G., Guiotto, A., Chilin, A., 2007 - 2010. Quinazoline derivatives as potential anticancer agents: a patent review. Expert Opin. Ther. Pat. 22 (3), 223–252.

Messenger, A.G., Rundegren, J., 2004. Minoxidil: mechanisms of action on hair growth. Br. J. Dermatol. 150 (2), 186–194.

Mfuh, A.M., Larionov, O.V., 2015. Heterocyclic N-oxides - an emerging class of therapeutic agents. Curr. Med. Chem. 22 (24), 2819–2857.

Nagelkerke, A., Span, P.N., 2016. Staining against phospho-H2AX (gamma-H2AX) as a marker for DNA damage and genomic instability in cancer tissues and cells. Adv. Exp. Med. Biol. 899, 1–10.

Nikolova, T., Dvorak, M., Jung, F., Adam, I., Kramer, E., Gerhold-Ay, A., Kaina, B., 2014. The γH2AX assay for genotoxic and nongenotoxic agents: comparison of H2AX phosphorylation with cell death response. Toxicol. Sci. 140, 103–117.

NRC, 2004. The development of science based Guidelines for laboratory animal Care. In: Proceedings of the November 2003 International Workshop. National Academy Press, Washington, DC.

OECD, 2009. Guideline for the Testing of Chemicals. Guideline 453: Combined Chronic

Toxicity\Carcinogenicity Studies. Adopted: 7 September 2009, Paris.

Pfizer, 1975. Genetic Toxicology Report CP-17,056 (Desoxycarbadox) Unpublished. (Submitted to WHO by Pfizer Central Research, Groton, CT, USA).

Prasad, S., Ravindran, J., Aggarwal, B.B., 2010. NF-kappaB and cancer: how intimate is this relationship. Mol. Cell. Biochem. 336, 25–37.

Redon, C.E., Nakamura, A.J., Martin, O.A., Parekh, P.R., Weyemi, U.S., Bonne, R.W.M., 2011. Recent developments in the use of g-H2AX as a quantitative DNA double-strand break biomarker. Aging 3, 168–174.

Redon, C.E., Weyemi, U., Parekh, P.R., Huang, D., Burrell, A.S., Bonner, W.M., 2012. γ-H2AX and other histone post-translational modifications in the clinic. Biochim. Biophys. Acta 1819, 743–756.

Reinert, H., 1976. Desoxycarbadox: Two Year Toxicity Study in Rats. WHO by Pfizer Central Research, Groton, CT, USA Unpublished.

Roe, F.J., Grant, G.A., Millican, D.M., 1967. Carcinogenicity of hydrazine and 1,1-di-methylhydrazine for mouse lung. Nature 216, 375–376.

Scarpato, R., Verola, C., Fabiani, B., Bianchi, V., Saggese, G., Federico, G., 2011. Nuclear damage in peripheral lymphocytes of obese and overweight Italian children as evaluated by the gamma-H2AX focus assay and micronucleus test. FASEB J. 25, 685–693.

Snyder, R.D., Green, J.W., 2001. A review of the genotoxicity of marketed pharmaceuticals. Mutat. Res. 488, 151–169.

Stebbins, R.B., Coleman, G.L., 1967. A Twenty-Six Month Chronic Toxicity Study of GS-6244 in Rats-Dose Levels of 100, 50 10, 5, or 0 Mg/kg. WHO by Pfizer Central Research, Groton, CT, USA Unpublished. Submitted to.

Steinhoff, D., Gunselmann, W., 1982. BAY VA 9391. Carcinogenicity Experiment with Oral Administration to Mice. Report No. 72388 (Revised), 100700 (Revised). Wuppertal-Elberfeld, FRG, pp. 12251 (revised). Unpublished report from Bayer AG.

Sykora, I., Vortel, V., 1986. Post-natal study of the carcinogenicity of cyadox and carbadox. Biol. Vet. Praha. 22, 53–62.

Thompson, C.M., Wolf, J.C., Elbekai, R.H., Paranjpe, M.G., Seiter, J.M., Chappell, M.A., Harris, M.A., 2015. Duodenal crypt health following exposure to Cr(VI): micronucleus scoring, gamma-H2AX immunostaining, and synchrotron X-ray fluorescence microscopy. Mutation Research. Gen. Toxicol. Environ. Mutagenesis 789–790, 61–66.

Toyoda, T., Cho, Y.M., Akagi, J., Mizuta, Y., Hirata, T., Nishikawa, A., Ogawa, K., 2015. Early detection of genotoxic urinary bladder carcinogens by immunohistochemistry for γ-H2AX. Toxicol. Sci. 148, 400–408.

Toyoda, T., Totsuka, Y., Matsushita, K., Morikawa, T., Miyoshi, N., Wakabayashi, K., Ogawa, K., 2018. γ-H2AX formation in the urinary bladder of rats treated with two norharman derivatives obtained from o-toluidine and aniline. J. Appl. Toxicol. 38 (4), 537–543.

Vicente, E., Perez-Silanes, S., Lima, L.M., Ancizu, S., Burguete, A., Solano, B., Villar, R., Aldana, I., Monge, A., 2009. Selective activity against Mycobacteriumtuberculosis of new quinoxaline 1,4-di-N-oxides. Bioorg. Med. Chem. 17, 385–389.

VICH, 2000. Safety Studies for Veterinary Drug Residues in Human Food: Genotoxicity Studies.

Wang, X., He, Q.H., Wang, Y.L., Ihsan, A., Huang, L.L., Zhou, W., Su, S.J., Liu, Z.L., Yuan, Z.H., 2011. A chronic toxicity study of cyadox in Wistar rats. Regul. Toxicol. Pharmacol. 59, 324–333.

Wang, X., Tan, Z., Pan, Y., Ihsan, A., Liu, Q., Huang, L., Cheng, G., Chen, D., Tao, Y., Liu, Z., Yuan, Z., 2015. Safety assessment of aditoprim acute, subchronic toxicity and mutagenicity studies. J. Appl. Toxicol. 35, 1415–1426.

Wang, X., Bai, Y., Cheng, G., Ihsan, A., Zhu, F., Wang, Y., Tao, Y., Chen, D., Dai, M., Liu, Z., Yuan, Z., 2016. Genomic and proteomic analysis of the inhibition of synthesis and secretion of aldosterone hormone induced by quinocetone in NCI-H295R cells. Toxicology 350–352, 1–14.

WHO, 1991a. World Health Organization. Toxicological Evaluation of Certain Veterinary Drug Residues in Food. Carbadox. WHO Food Additives Series, No., vol. 27 INCHEM No. 700 on.

WHO, 1991b. World Health Organization. Toxicological Evaluation of Certain Veterinary Drug Residues in Food. Olaquindox. WHO Food Additives Series, No, vol. 27 INCHEM no. 701 on.

Wu, Y., Yu, H., Wang, Y., et al., 2007. Development of a high-performance liquid chromatography method for the simultaneous quantification of quinoxaline-2-carboxylic acid and methyl-3-quinoxaline-2-carboxylic acid in animal tissues. J. Chromatogr. A 1146 (1), 1–7.

Wu, H., Li, L., Shen, J., Wang, Y., Liu, K., Zhang, S., 2012. In vitro metabolism of cyadox in rat, chicken and swine using ultra-performance liquid chromatography quadrupole time-of-flight mass spectrometry. J. Pharmaceut. Biom. 67–68, 175–185.

Yang, W., Fu, J., Xiao, X., Yan, H., Bao, W., Wang, D., Hao, L., Nussler, A.K., Yao, P., Liu, L., 2013. Quinocetone triggers oxidative stress and induces cytotoxicity and genotoxicity in human peripheral lymphocytes of both genders. J. Sci. Food Agric. 93, 1317–1325.

Yoshimura, H., 2002. Teratogenic assessment of carbadox in rats. Toxicol. Lett. 129 (1–2), 115–118.

Yu, M., Wang, D., Xu, M.J., Liu, Y., Wang, X., Liu, J., Yang, X.F., Yao, P., Yan, H., Liu, L.G., 2014. Quinocetone-induced Nrf2/HO-1 pathway suppression aggravates hepatocyte damage of Sprague-Dawley rats. Food Chem. Toxicol. 69, 210–219.

Ze, Y., Zheng, L., Zhao, X., Gui, S., Sang, X., Su, J., Guan, N., Zhu, L., Sheng, L., Hu, R., Cheng, J., Cheng, Z., Sun, Q., Wang, L., Hong, F., 2013. Molecular mechanism of titanium dioxide nanoparticles-induced oxidative injury in the brain of mice. Chemosphere 92, 1183–1189.

Zhao, D., Wang, C., Tang, S., et al., 2014. Reactive oxygen species-dependent JNK downregulated olaquindox-induced autophagy in HepG2 cells. J. Appl. Toxicol. 35 (7), 709–716.